Nonlinear Energy Harvesting Models in Wireless Information and Power Transfer

Panos N. Alevizos, Georgios Vougioukas, and Aggelos Bletsas
School of ECE, Technical Univ. of Crete, Kounoupidiana Campus, Greece 73100
e-mail: {palevizos, gevougioukas}@isc.tuc.gr, aggelos@telecom.tuc.gr

***Abstract*—This work compares different linear and nonlinear RF energy harvesting models, including limited or unlimited sensitivity, for simultaneous wireless information and power transfer (SWIPT). The probability of successful SWIPT reception under a family of RF harvesting models is rigorously quantified, using state-of-the-art rectifiers in the context of commercial RFIDs. A significant portion of SWIPT literature uses oversimplified models that do not account for limited sensitivity or nonlinearity of the underlying harvesting circuitry. This work demonstrates that communications signals are not always appropriate for simultaneous energy transfer and concludes that for practical SWIPT studies, the inherent non-ideal characteristics of the harvester should be carefully taken into account; specific harvester's modeling methodology is also offered.**

I. Introduction

Intense research has been devoted the last years on simultaneous wireless information and power transfer (SWIPT). The main concept in far field SWIPT systems is the exploitation of the communication signals for radio frequency (RF) energy harvesting, typically with rectennas, i.e., antenna and rectifier(s). The latter perform the required RF-to-DC conversion, including one (or more) diode(s). The main problem in far field RF energy harvesting is the limited sensitivity of the circuit, currently in the order of -35 dBm to -25 dBm, with slow improvement by a factor of 2 every approximately 5 years [?]. Such power levels below which energy transfer cannot be performed, are orders of magnitude higher than current communications circuits sensitivity, which may reach values as low as -130 dBm to -80 dBm, depending on bandwidth. Thus, signals appropriate for communications may not be *simultaneously* suitable for energy transfer [?], [?].

Another major issue in the SWIPT literature is the adoption of oversimplified RF harvesting models, which either exhibit a linear relationship between input RF and output harvested power or assume unlimited sensitivity. Rectennas, due to the presence of diode(s), exhibit a highly nonlinear behavior, with limited sensitivity, due to the need for bias. Despite the vast amount of literature in the wireless communications theory community that adheres to the above assumptions, exceptions have only recently started to emerge; for example, work in [?], [?] utilized convex optimization techniques to optimize the parameters of multi-tone waveforms, which improve RF harvesting efficiency compared to single-tone, while taking into account the nonlinearity of the rectifier. Other nonlinear RF harvesting models have been recently proposed, which however miss the limited sensitivity issue and will be discussed subsequently.

Therefore, there is a strong need to evaluate different RF harvesting models, taking into account *both* harvesting sensitivity *and* nonlinearity, as well as facts from the relevant microwave literature. Radio frequency identification (RFID) technology is the most prominent example of SWIPT, with significant prior art, as well as commercial interest. This work compares different linear and nonlinear energy harvesting models for SWIPT, taking also into account limited or unlimited sensitivity; comparisons are performed based on real, state-of-the-art rectifiers [?] in RFID, using backscatter communications. It is found that neglecting harvester's nonlinearity and limited sensitivity may offer misleading results.

II. Signal Model

Backscatter radio/RFID technology is the most prominent example of SWIPT. A monostatic, single-antenna reader topology is examined with reader and tag, depicted in Fig. 1. In that case, the illuminating carrier emitter and the receiver of the tag-backscattered signal is the same, full-duplex unit, a.k.a. the reader; the latter is equipped with a single antenna serving both reception and transmission, using an appropriate duplexer, the circulator. Thus, path-loss and small-scale fading are the same for both reader-to-tag (downlink) and tag-to-reader (uplink) links. Both links are subject to large-scale fading, where the path-gain at tag-to-reader distance d is given by:

$$\mathsf{L} \equiv \mathsf{L}(d) = \left(\frac{\lambda}{4\pi d_0}\right)^2 \left(\frac{d_0}{d}\right)^{\nu}, \tag{1}$$

where d_0 is a reference distance (assumed unit thereinafter), λ is the wavelength and ν is the path loss exponent.

Flat fading is assumed due to relatively small communication bandwidth. Thus, small-scale fading coefficient, for both downlink and uplink is given by $h = a\mathrm{e}^{-\mathrm{j}\phi}$. Due to potential strong line-of-sight (LoS), Nakagami small-scale fading is assumed with $\mathbb{E}\left[a^2\right] = 1$ and Nakagami parameter $\mathtt{M} \geq \frac{1}{2}$ [?, p. 79]. The special cases of Rayleigh fading and no fading ($a = 1$) are obtained for $\mathtt{M} = 1$ and $\mathtt{M} = \infty$, respectively.

Assuming the reader emits an unmodulated carrier with transmit power P_{R} and frequency F_{c}, the impinged signal at the tag signal can be expressed as follows:

$$\mathsf{c}_{\mathrm{T}}(t) = \sqrt{2\,\mathsf{L}\,\mathsf{P}_{\mathrm{R}}}\,\Re\{h\,\mathrm{e}^{\mathrm{j}2\pi F_{\mathrm{c}} t}\}. \tag{2}$$

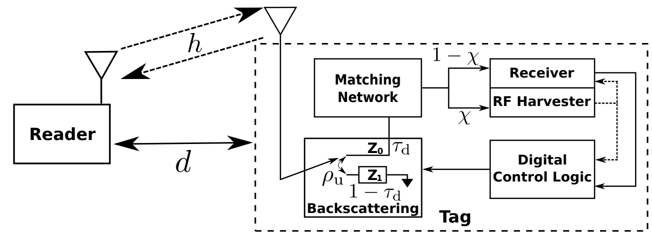

Fig. 1. Monostatic backscatter architecture consisting of a reader and a passive (i.e., batteryless) RFID tag. Reader acts as carrier emitter, as well as receiver of tag reflected/backscattered information.

The received power at the tag is then given by:

$$P_{\rm in} = \mathsf{L}\,\mathsf{P}_{\rm R}\,|h|^2 = \mathsf{L}\,\mathsf{P}_{\rm R}\,a^2. \tag{3}$$

According to the above, $P_{\rm in}$ follows Gamma distribution ($\mathbb{E}\big[a^2\big] = 1$): $\mathsf{f}_{P_{\rm in}}(x) = \left(\frac{\mathtt{M}}{\mathsf{L}\,\mathsf{P}_{\rm R}}\right)^{\mathtt{M}} \frac{x^{\mathtt{M}-1}}{\Gamma(\mathtt{M})}\,\mathsf{e}^{-\frac{\mathtt{M}}{\mathsf{L}\,\mathsf{P}_{\rm R}}x},\ x \geq 0$, where $\left(\mathtt{M}, \frac{\mathsf{L}\,\mathsf{P}_{\rm R}}{\mathtt{M}}\right)$ the shape and scale parameter, respectively, and $\Gamma(x) = \int_0^\infty t^{x-1}\mathsf{e}^{-t}\mathsf{d}t$ is the Gamma function.

III. RFID Tag Operation

The RFID tag does not include any power-demanding signal conditioning units, e.g., amplifiers, mixers or oscillators (Fig. 1). Instead, communication is achieved by varying the reflection coefficient between tag antenna and its termination loads, using a RF switch. Binary modulation is achieved with two different reflection coefficients (i.e., two different termination loads Z_0, Z_1). This operation results to modulation of tag information on top of the reader illuminating signal, reflected (from the tag) back to the reader, in an ultra low-power fashion.

A. RF Harvesting & Tag Powering

In order for the RFID tag to operate, power must be harvested from the impinged, reader-generated signal. Input power must be above the tag harvester sensitivity $\mathtt{P}_{\rm sen}$, i.e., $P_{\rm in} > \mathtt{P}_{\rm sen}$. $\mathtt{P}_{\rm sen}$ is a crucial parameter in backscatter communication with passive tags, due to the fact that state-of-the-art, far field RF harvesters offer limited sensitivity.

Work in [**?**] established that a high-order polynomial in the dBm scale can be safely considered as ground truth model for harvesting efficiency function; thus, harvested power can be modeled as a function of input power x as follows:

$$\mathsf{p}(x) = \begin{cases} 0, & x \in [0, \mathtt{P}_{\rm sen}) \\ \left(w_0 + \sum_{i=1}^{W} w_i (10\log_{10}(x))^i\right) \cdot x, & x \in [\mathtt{P}_{\rm sen}, \mathtt{P}_{\rm sat}], \\ \mathsf{p}(\mathtt{P}_{\rm sat}), & x \geq \mathtt{P}_{\rm sat}, \end{cases} \tag{4}$$

where x and $\mathsf{p}(x)$ take values in mWatt, while the quantity $\left(w_0 + \sum_{i=1}^{W} w_i (10\log_{10}(x))^i\right)$ is the harvesting efficiency function, with W being the degree of the polynomial and $\{w_i\}_{i=0}^{W}$ the corresponding coefficients. For the analysis below we assume that function $\mathsf{p}(x)$ is continuous and increasing in $[\mathtt{P}_{\rm sen}, \mathtt{P}_{\rm sat}]$. As shown in [**?**], the parameters $\{w_i\}_{i=0}^{W}$ in Eq. (4) can be obtained directly from harvesters' data using standard convex optimization fitting methods.

Several models have been proposed in order for the harvested power to be mathematically described. These models are summarized below:

1) Linear Model (L): Single parameter model, where the harvested power can be expressed as $\mathsf{p}_1(x) \triangleq \eta_{\rm L} x,\ x \geq 0$. This is the most utilized model in SWIPT literature, it's linear and does not account for harvesters' sensitivity.

2) Constant Linear (CL): Linear model with the addition of taking into account the sensitivity of the harvester. According to that model, harvested power is expressed as $\mathsf{p}_2(x) = \eta_{\rm CL} \cdot (x - \mathtt{P}_{\rm sen})$ for $x \in [\mathtt{P}_{\rm sen}, \infty)$ and zero in the rest of its domain; $\eta_{\rm CL}$ is the constant harvesting efficiency.

3) Nonlinear Normalized Sigmoid: The model was proposed in [**?**] and assumes $\mathtt{P}_{\rm sen} = 0$, i.e., it does not account for harvesters' sensitivity. The harvested power is expressed as:

$$\mathsf{p}_3(x) \triangleq \frac{\frac{\mathsf{c}_0}{1+\exp(-\mathsf{a}_0(x-\mathsf{b}_0))} - \frac{\mathsf{c}_0}{1+\exp(\mathsf{a}_0\,\mathsf{b}_0)}}{1 - \frac{1}{1+\exp(\mathsf{a}_0\,\mathsf{b}_0)}}. \tag{5}$$

The shape of $\mathsf{p}_3(x)$ is determined by three real numbers a_0, b_0, and c_0. A similar, sigmoid model accounting however for $\mathtt{P}_{\rm sen}$, was proposed in [**?**], where the harvested power is modeled as:

$$\mathsf{p}_4(x) \triangleq \max\left\{\frac{\mathsf{c}_1}{\exp(-\mathsf{a}_1\mathtt{P}_{\rm sen}+\mathsf{b}_1)}\left(\frac{1+\exp(-\mathsf{a}_1\mathtt{P}_{\rm sen}+\mathsf{b}_1)}{1+\exp(-\mathsf{a}_1 x+\mathsf{b}_1)} - 1\right), 0\right\}.$$

4) Second Order Polynomial: In [**?**] a model based on a second degree polynomial in milliWatt domain has been suggested. Following that model, harvested power can be expressed as $\mathsf{p}_5(x) \triangleq \mathsf{a}_2\,x^2 + \mathsf{b}_2\,x + \mathsf{c}_2$. The above model does not account for $\mathtt{P}_{\rm sen}$. In order to encompass the effect of sensitivity, $\mathsf{p}_5(\cdot)$ can be modified as

$$\mathsf{p}_6(x) \triangleq \mathsf{a}_3(x - \mathtt{P}_{\rm sen})^2 + \mathsf{b}_3(x - \mathtt{P}_{\rm sen}). \tag{6}$$

The parameters of the model in Eq. (6) are a_3, b_3 and $\mathtt{P}_{\rm sen}$.

5) Piecewise Linear Model: Given a set of $J+1$ data pairs of input power and corresponding harvested power, denoted as $\{q_j\}_{j=0}^{J}$ and $\{v_j\}_{j=0}^{J}$, respectively, slopes $l_j \triangleq \frac{v_j - v_{j-1}}{q_j - q_{j-1}}$, $j \in [J]$ are defined, where $[J] \triangleq \{1, 2, \ldots, J\}$. Modeling sensitivity and saturation characteristics is done through points $q_0 = \mathtt{P}_{\rm sen}$ and $q_J = \mathtt{P}_{\rm sat}$. Having those slopes, the harvested power is given by:

$$\mathsf{p}_7(x) \triangleq \begin{cases} 0 & x \in [0, q_0], \\ l_j(x - q_{j-1}) + v_{j-1}, & x \in (q_{j-1}, q_j],\ \forall j \in [J], \\ v_J, & x \in [q_J, \infty). \end{cases} \tag{7}$$

Function $\mathsf{p}_7(x)$ is defined using $2(J+1)$ real numbers, easily available from harvesters' specifications; thus, determining $\mathsf{p}_7(x)$ is straightforward, without any tuning.

It should be noted that the last model can potentially model energy harvesting from other sources, other than RF. For instance, if photodiodes are used in order to harvest energy from either ambient or solar light, the proposed model can

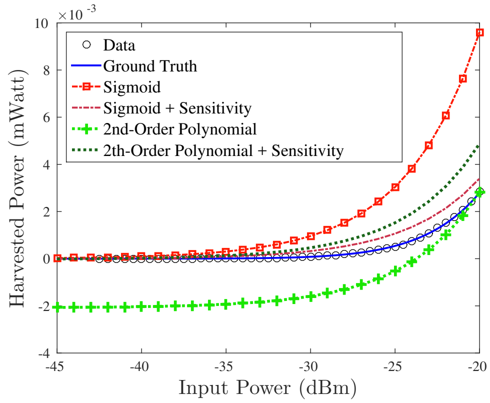

Fig. 2. Harvested power (in milliWatt) versus input power (in dBm) for the harvester proposed in [?] using nonlinear harvested power function $\mathsf{p}_n(\cdot)$, $n = 3, 4, 5, 6$, as well as for the ground truth model in Eq. (4). Input power range within $[-45, -20]$ dBm.

describe the harvested power, as a function of illuminance (measured in lux). This statement is based on the nonlinear behavior of the photodiodes (similarly to RF rectification circuits), when used as harvesting elements (for example see work in [?], [?]).

6) Diode-Based Hardware-Specific Model: In [?], [?] a hardware-specific, nonlinear model is proposed. That model is based on the physics of the diode and links the output DC current (and therefore DC power) to the input signal (power and shape). For a specific RF energy harvesting circuit with one or multiple diode, the output DC current is expressed as:

$$i_{\text{out}} = \sum_{i=0}^{\mathtt{n}_0} \kappa_i \, \mathtt{R}_{\text{a}}^{i/2} \, \mathbb{E}[\mathsf{c}_{\text{T}}(t)^i] \tag{8}$$

where diode-dependent parameter κ_i depends on (i) the reverse bias saturation current, (ii) the thermal voltage, and (iii) the ideality factor of the diode, $\mathtt{R}_{\text{a}}$ is the impedance, and $\mathtt{n}_0$ is a truncation parameter. Note that the above model depends on the hardware characteristics of the rectifier and the modeling changes for different type of RF harvesters.

Fig. 2 illustrates the harvested power (in mWatt) versus input power (in dBm) for the harvester proposed in [?] using as ground truth the specification data; the nonlinear model in Eq. (4) adheres to the data; the rest of the nonlinear harvested power function $\mathsf{p}_n(\cdot)$, $n = 3, 4, \ldots, 6$, discussed above, are also depicted (using Matlab's fitting toolbox). Due to strong nonlinearity, the linear models were omitted from the plot.

During normal operation, tags' antenna is terminated at load Z_0 (absorbing state, see Fig. 1) for a time fraction of τ_{d} while for the rest $1 - \tau_{\text{d}}$, antenna is connected to Z_1 (reflection state). Given that the tag is at Z_0, a portion χ of the received power is destined solely for energy harvesting, i.e., $\zeta_{\text{har}} = \chi\,\tau_{\text{d}} \in (0, 1)$ percentage of input power is dedicated for RF energy harvesting. The rest $(1-\chi)\tau_{\text{d}}$, is exploited for downlink communication purposes.

Thus, in order for the tag to operate, the total harvested power $\mathsf{p}(\zeta_{\text{har}} P_{\text{in}})$ must be greater than the tag overall power consumption $\mathtt{P}_{\text{c}}$. This is critical, given the fact that batteryless RFID tags typically incorporate no energy storage element, e.g., (super)capacitor, due to size and cost limitations.

B. Backscatter Communication

As stated earlier, the tag alters the load terminating its antenna using a switch. Load Z_0 is, by construction, designed to match antennas' impedance. Thus, when antenna is terminated at Z_0, the load absorbs (ideally, if perfectly matched) all the power offered by the impinged signal. When the antenna is terminated at Z_1, a fraction $\rho_{\text{u}} \leq 1 - \tau_{\text{d}}$ of the impinged power is used for uplink scatter radio operation. Parameter ρ_{u} depends on the tag scattering efficiency (which also incorporates non-idealities from the above model). Modified reflection coefficient [?] Γ_i, when the antenna is terminated at Z_i, $i \in \{0, 1\}$, is given by $\Gamma_i = \frac{Z_i - \mathtt{Z}_{\text{a}}^*}{Z_i + \mathtt{Z}_{\text{a}}}$, where $\mathtt{Z}_{\text{a}}$ antenna's impedance. The baseband equivalent of the tag-backscattered signal can be expressed as [?] $\mathtt{A}_s - \Gamma_i$, which in turn depends on the (load-independent) tag antenna structural mode $\mathtt{A}_s$ and the transmitted bit i; the backscattered baseband signal, for a duration of N tag bits, is given by [?]:

$$\mathsf{b}(t) = \sqrt{\mathsf{L}\rho_{\text{u}}\mathtt{P}_{\text{R}}}\, h\left(\mathtt{A}_s - \Gamma_0 + \Delta\Gamma \sum_{n=1}^{N} \mathsf{s}_{b_n}(t-(n-1)T)\right), \tag{9}$$

where, $\Delta\Gamma \triangleq (\Gamma_0 - \Gamma_1)$, $b_n \in \{0, 1\}$ is the n-th reflected bit, while function $\mathsf{s}_{b_n}(\cdot)$ is the backscattered signal basis function, of duration T, when bit b_n is transmitted.

In order to a) balance the time for which the tag is absorbing energy, independently of the tag's data bits, and b) avoid *ghost* tag reception, i.e., reader misinterpreting thermal noise as tag information, a *line* code is used in commercial GEN2 RFIDs [?], selecting between FM0 and Miller. Under FM0 coding, observing $2T$ signal duration for each bit (of duration T) suffices for BER-optimal, coherent (differential) detection and $\mathsf{s}_{b_n}(\cdot)$ is a $T/2$-shifted waveform found in [?, Eq. (3)].

After DC-blocking, assuming perfect synchronization, the optimal demodulator projects the received signal onto the basis functions subspace using two correlators. The discrete baseband signal, at the output of the correlators, follows [?, Theorem 1]:

$$\mathbf{y}_n = g\,\mathbf{s}_n + \mathbf{w}_n, \;\; n = 1, 2, \ldots, N, \tag{10}$$

where $g \triangleq \mathsf{L}\sqrt{\rho_{\text{u}}\mathtt{P}_{\text{R}}}\, h^2\,(\Gamma_0 - \Gamma_1)$, and $\mathbf{s}_n$ is the vector representation for the n-th transmitted signal. For RFID systems, which employ $T/2$-shifted FM0 line-coding, $\mathbf{s}_n \in \left\{[1 \;\; 0]^\top, [0 \;\; 1]^\top\right\}$ and $\mathbf{w}_n \sim \mathcal{CN}(\mathbf{0}_2, \sigma^2\,\mathbf{I}_2)$ [?], [?], with σ^2 denoting the variance of each noise component.

IV. Reader

A. Bit Error Rate (BER)

Assuming coherent ML differential detection (with signal of $2T$ duration, given known channel g), the conditional bit error probability for the baseband signal in Eq. (10) follows from [?], [?]:

$$\mathbb{P}(\text{error}|g) = 2\,\mathsf{Q}\left(\frac{|g|}{\sigma}\right)\left(1 - \mathsf{Q}\left(\frac{|g|}{\sigma}\right)\right), \tag{11}$$

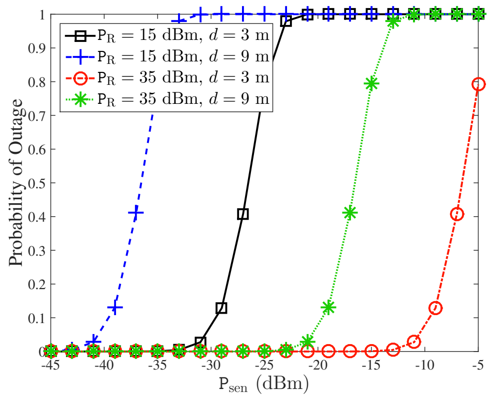

Fig. 3. Probability of sensitivity outage event as a function of tag's harvesting sensitivity. The path-loss model of Eq. (1) is employed with $\nu = 2.1$, $\lambda = 0.3456$ and $\mathtt{M} = 5$.

where $\mathsf{Q}(x) = \frac{1}{\sqrt{2\pi}} \int_x^{\infty} \mathrm{e}^{-\frac{t^2}{2}} \mathrm{d}t$ is the Q-function. Interestingly, a similar expression applies to Miller line coding, when the receiver performs coherent (ML) bit-by-bit detection.

B. Outage Scenarios

The reader receives successfully the RFID tag's information when: a) the input RF power at the tag antenna is above RF harvesting sensitivity, and b) the harvested power is above tag's power consumption, given that the RFID tag does not include energy storage elements, and c) BER at the reader is below a threshold β. Probability of these events is analyzed below.

1) Outage due to limited harvesters' sensitivity: Considering the definition of input power in Eq. (3), tag's harvesting sensitivity outage metric is defined as follows:

$$\mathbb{P}(\mathcal{A}) \triangleq \mathbb{P}(P_{\text{in}} \leq \mathtt{P}_{\text{sen}}) = \mathsf{F}_{P_{\text{in}}}(\mathtt{P}_{\text{sen}}), \tag{12}$$

where $\mathsf{F}_{P_{\text{in}}}(\cdot)$ is the cumulative distribution function (CDF) of P_{in}. Eq. (12) mathematically describes the probability that the input power P_{in} at the RFID tag antenna (which depends on the wireless channel/fading), is below tag RF harvester's sensitivity $\mathtt{P}_{\text{sen}}$. Such outage event represents the fraction of time the tag's rectenna cannot harvest RF energy due to inadequate input RF power. Under Nakagami fading such outage is given by:

$$\mathsf{F}_{P_{\text{in}}}(\mathtt{P}_{\text{sen}}) = 1 - \int_{\mathtt{P}_{\text{sen}}}^{\infty} \mathsf{f}_{P_{\text{in}}}(y)\mathsf{d}y = 1 - \frac{\Gamma\left(\mathtt{M}, \frac{\mathtt{M}}{\mathtt{L}\,\mathtt{P}_{\text{R}}}\mathtt{P}_{\text{sen}}\right)}{\Gamma(\mathtt{M})}, \tag{13}$$

where $\Gamma(\alpha, z) = \int_z^{\infty} t^{\alpha-1}\mathrm{e}^{-t}\mathrm{d}t$. At this point, it must be emphasized that RF receiver sensitivity for communication purposes can obtain values from -80 dBm or less, while state-of-the-art rectennas offer harvesting sensitivity in the order of around -40 to -35 dBm [**?**]. Clearly, *signals useful for communication may not be useful for power transfer*.

Fig. 3 examines Eq. (12) as a function of tag RF harvester's sensitivity. It can be clearly seen that less-sensitive RF harvesters, suffer from higher outage probabilities. RF harvesting sensitivity is commonly neglected in SWIPT research, even though it tremendously impacts the *power transfer* part and thus, overall performance [**?**].

2) Outage due to limited power consumption: When input power is above tag's harvesting sensitivity, the next type of outage is when the harvested power, $\mathsf{p}(\zeta_{\text{har}}\, P_{\text{in}})$ is *not enough*, i.e., below tag's power consumption $\mathtt{P}_{\text{c}}$:

$$\mathbb{P}(\mathsf{p}(\zeta_{\text{har}}\, P_{\text{in}}) \leq \mathtt{P}_{\text{c}}), \tag{14}$$

which depends on (a) fading and input power at the tag, (b) the type of the RF harvester, and (c) tag's power consumption $\mathtt{P}_{\text{c}}$; such probability describes the fraction of time the harvested power is not adequate for tag powering and is critical for devices that cannot store harvested energy. If $\mathsf{p}(\cdot)$ is strictly increasing and continuous around $\mathtt{P}_{\text{c}}$, the event in Eq. (14) can be simplified as follows:

$$\mathbb{P}(\mathcal{B}) \triangleq \mathbb{P}\left(P_{\text{in}} \leq \frac{\mathsf{p}^{-1}(\mathtt{P}_{\text{c}})}{\zeta_{\text{har}}}\right) = \mathsf{F}_{P_{\text{in}}}\left(\frac{\mathsf{p}^{-1}(\mathtt{P}_{\text{c}})}{\zeta_{\text{har}}}\right), \tag{15}$$

where $\mathsf{p}^{-1}(\mathtt{P}_{\text{c}})$ is the inverse function of $\mathsf{p}(\cdot)$ at point $\mathtt{P}_{\text{c}}$.

3) Information Outage: RFID tag information outage at the reader is defined when BER in Eq. (11) is below a predefined precision β. Setting $\mathsf{R}(x) \triangleq 2\,\mathsf{Q}(x)\,(1 - \mathsf{Q}(x)),\ x \in (0, \infty)$, this event can be mathematically expressed as [**?**]:

$$\mathbb{P}(\mathcal{C}) \triangleq \mathbb{P}\left(P_{\text{in}} \leq \frac{\sqrt{\mathtt{P}_{\text{R}}}\,\sigma\,\mathsf{R}^{-1}(\beta)}{|\Gamma_0 - \Gamma_1|\sqrt{\rho_{\text{u}}}}\right) = \mathsf{F}_{P_{\text{in}}}\left(\frac{\sqrt{\mathtt{P}_{\text{R}}}\,\sigma\,\mathsf{R}^{-1}(\beta)}{|\Gamma_0 - \Gamma_1|\sqrt{\rho_{\text{u}}}}\right), \tag{16}$$

where $\mathsf{R}^{-1}(x) = \mathsf{Q}^{-1}\left(\frac{1-\sqrt{1-2\,x}}{2}\right)$, defined for $x \in (0, 0.5)$ and $\mathsf{Q}^{-1}(\cdot)$ is the inverse of Q-function.

C. Probability Of Successful Reception

Tag information is unsuccessfully received when *either* of previously discussed events $\mathcal{A}$, $\mathcal{B}$, $\mathcal{C}$ occurs. Assuming that function $\mathsf{p}(\cdot)$ is strictly increasing and continuous around $\mathtt{P}_{\text{c}}$ and denoting for an event $\mathcal{D}$ its complement as $\mathcal{D}^{\complement}$, the probability of unsuccessful SWIPT reception, denoted as event $\mathcal{F}$, can be expressed as:

$$\begin{aligned}\mathbb{P}(\mathcal{F}) &= 1 - \mathbb{P}(\mathcal{F}^{\complement}) = 1 - \mathbb{P}(\mathcal{A}^{\complement} \cap \mathcal{B}^{\complement} \cap \mathcal{C}^{\complement}) \\ &= 1 - \mathbb{P}(P_{\text{in}} > \theta_{\mathcal{F}}) = \mathsf{F}_{P_{\text{in}}}(\theta_{\mathcal{F}}),\end{aligned} \tag{17}$$

where $\theta_{\mathcal{F}} \triangleq \max\left\{\mathtt{P}_{\text{sen}}, \frac{\mathsf{p}^{-1}(\mathtt{P}_{\text{c}})}{\zeta_{\text{har}}}, \frac{\sqrt{\mathtt{P}_{\text{R}}}\,\sigma\,\mathsf{R}^{-1}(\beta)}{|\Gamma_0 - \Gamma_1|\sqrt{\rho_{\text{u}}}}\right\}$. Consequently, successful SWIPT reception at the reader, under Nakagami fading, is given in closed form as follows:

$$\mathbb{P}(\text{SWIPT success}) \equiv \mathbb{P}(\mathcal{F}^{\complement}) = \frac{\Gamma\left(\mathtt{M}, \frac{\mathtt{M}}{\mathtt{L}\,\mathtt{P}_{\text{R}}}\theta_{\mathcal{F}}\right)}{\Gamma(\mathtt{M})}. \tag{18}$$

V. Numerical Results

For the simulation results the path-loss model of Eq. (1) is considered with $\nu = 2.3$ and $\lambda = 0.3456$ (UHF carrier frequency), and tag antenna reflection coefficients Γ_0 and Γ_1 satisfying $|\Gamma_0 - \Gamma_1| = 1$. The ultra-sensitive harvester in [**?**] is tested using parameters $\tau_{\text{d}} = 0.5$, $\chi = 0.5$, $\rho_{\text{u}} = 0.01$ for RF harvesting and backscattering at the tag, while BER threshold

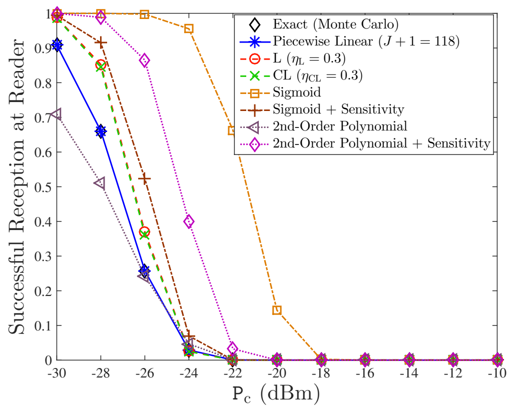

Fig. 4. Probability of successful SWIPT reception at reader, as a function of tag power consumption-Strong LoS.

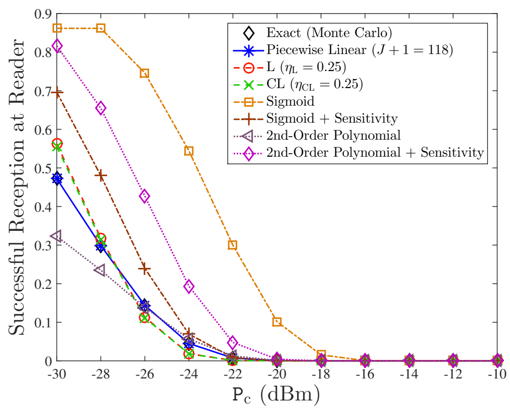

Fig. 5. Probability of successful SWIPT reception at reader, as a function of tag power consumption-non LoS.

is set $\beta = 10^{-5}$; variance of noise at the reader was set to 10^{-11}.

Fig. 4 depicts probability of successful SWIPT reception at the reader, as a function of tag's power consumption, in a strong LoS scenario (Nakagami parameter $\mathtt{M} = 10$), $d = 4$ m, and $P_R = 1$ Watt. Fig. 5 examines the same relationship in a non-LoS scenario ($\mathtt{M} = 2$), $d = 7$ m, and $P_R = 2.5$ Watt.

Both figures clearly show that the performance of the piecewise linear model $\mathsf{p}_7(\cdot)$ coincides with the exact (ground-truth, $\mathsf{p}(\cdot)$), data-driven model. The performance of $\mathsf{p}_1(\cdot)$ (L), as well as $\mathsf{p}_2(\cdot)$ (CL) model deviate from reality, even though the best values for the efficiency parameters were utilized (i.e., values that offered performance as close as possible to the ground-truth model). Both nonlinear sigmoid models tend to overestimate the event while the one incorporating sensitivity, offers closer-to-reality results in the LoS scenario and deviates further in the non-LoS scenario. Finally, the second-order polynomial $\mathsf{p}_5(\cdot)$ underestimates performance, with performance gap that depends on the scenario and tag's power consumption, whereas energy harvesting model $\mathsf{p}_6(\cdot)$ overestimates the harvested power. In short, SWIPT research requires *accurate* energy harvesting models, otherwise misleading conclusions are unavoidable.

VI. Conclusion

SWIPT research should always take into account all the non-ideal characteristics of the RF energy harvesting system; otherwise, oversimplification due to overlooking fundamentals from electronics and microwave engineering may lead to impractical results. This work studied the sensitivity and the nonlinearity of the harvester. Impact of other modules, present in the RF harvesting chain (e.g., boost converter/maximum power point tracking-MPPT), should be also examined.

Acknowledgment

This research is implemented through the Operational Program "Human Resources Development, Education and Lifelong Learning" and is co-financed by the European Union (European Social Fund) and Greek national funds.

References

[1] G. D. Durgin, "RF thermoelectric generation for passive RFID," in *Proc. IEEE RFID*, Orlando, FL, May 2016, pp. 1–8.

[2] P. Alevizos, "Intelligent scatter radio, RF harvesting analysis, and resource allocation for ultra-low-power internet-of-things," Ph.D. dissertation, School of ECE, Technical University of Crete, Chania, Greece, 2017, advisor: A. Bletsas.

[3] P. N. Alevizos and A. Bletsas, "Sensitive and nonlinear far field RF energy harvesting in wireless communications," *IEEE Trans. Wireless Commun.*, 2018, accepted, to appear. [Online]. Available: https://arxiv.org/pdf/1707.07041.pdf

[4] B. Clerckx and E. Bayguzina, "Waveform design for wireless power transfer," *IEEE Trans. Signal Processing*, vol. 64, no. 23, pp. 6313–6328, Dec. 2016.

[5] B. Clerckx, "Wireless information and power transfer: Nonlinearity, waveform design and rate-energy tradeoff," *IEEE Trans. Signal Processing*, vol. 66, no. 4, pp. 847–862, Feb. 2018.

[6] S. D. Assimonis, S.-N. Daskalakis, and A. Bletsas, "Sensitive and efficient RF harvesting supply for batteryless backscatter sensor networks," *IEEE Trans. Microwave Theory Tech.*, vol. 64, no. 4, pp. 1327–1338, Apr. 2016.

[7] A. Goldsmith, *Wireless Communications*. New York, NY, USA: Cambridge University Press, 2005.

[8] E. Boshkovska, D. W. K. Ng, N. Zlatanov, and R. Schober, "Practical non-linear energy harvesting model and resource allocation for SWIPT systems," *IEEE Commun. Lett.*, vol. 19, no. 12, pp. 2082–2085, Dec. 2015.

[9] S. Wang, M. Xia, K. Huang, and Y. C. Wu, "Wirelessly powered two-way communication with nonlinear energy harvesting model: Rate regions under fixed and mobile relay," *IEEE Trans. Wireless Commun.*, vol. 16, no. 12, pp. 8190–8204, Dec. 2017.

[10] X. Xu, A. Özcelikkale, T. McKelvey, and M. Viberg, "Simultaneous information and power transfer under a non-linear RF energy harvesting model," in *Proc. IEEE Int. Conf. Communications*, Paris, France, May 2017, pp. 179–184.

[11] N. J. Guilar, T. J. Kleeburg, A. Chen, D. R. Yankelevich, and R. Amirtharajah, "Integrated solar energy harvesting and storage," *IEEE Trans. VLSI Syst.*, vol. 17, no. 5, pp. 627–637, May 2009.

[12] E. G. Fong, N. J. Guilar, T. J. Kleeburg, H. Pham, D. R. Yankelevich, and R. Amirtharajah, "Integrated energy-harvesting photodiodes with diffractive storage capacitance," *IEEE Trans. VLSI Syst.*, vol. 21, no. 3, pp. 486–497, Mar. 2013.

[13] A. Bletsas, A. G. Dimitriou, and J. Sahalos, "Improving backscatter radio tag efficiency," *IEEE Trans. Microwave Theory Tech.*, vol. 58, no. 6, pp. 1502 – 1509, Jun. 2010.

[14] J. Kimionis, A. Bletsas, and J. N. Sahalos, "Bistatic backscatter radio for power-limited sensor networks," in *Proc. IEEE Global Commun. Conf. (Globecom)*, Atlanta, GA, Dec. 2013, pp. 353–358.

[15] *EPC Radio-Frequency Identity Protocols, Class-1 Generation-2 UHF RFID Protocol for Communications at 860 MHZ-960 MHZ.* EPC Global, 2008, version 1.2.0.

[16] N. Kargas, F. Mavromatis, and A. Bletsas, "Fully-coherent reader with commodity SDR for Gen2 FM0 and computational RFID," *IEEE Wireless Commun. Lett.*, vol. 4, no. 6, pp. 617–620, Dec. 2015.

[17] N. Fasarakis-Hilliard, P. N. Alevizos, and A. Bletsas, "Coherent detection and channel coding for bistatic scatter radio sensor networking," *IEEE Trans. Commun.*, vol. 63, pp. 1798–1810, May 2015.

[18] M. Simon and D. Divsalar, "Some interesting observations for certain line codes with application to RFID," *IEEE Trans. Commun.*, vol. 54, no. 4, pp. 583–586, Apr. 2006.

[19] P. N. Alevizos, K. Tountas, and A. Bletsas, "Multistatic scatter radio sensor networks for extended coverage." [Online]. Available: arxiv.org/pdf/1706.03091.pdf